17th World Conference on Earthquake Engineering, 17WCEE
Sendai, Japan - September 13th to 18th 2020

JAPANESE RECENT EXPERIMENTAL STUDIES ON ULTIMATE BEHAVIOR OF CONCRETE PILES AND PILE CAPS

S. Kono[(1)], T. Mukai[(2)], K. Kobayashi[(3)], O. Kaneko[(4)], S. Kishida[(5)], T. Komuro[(6)], T. Obara[(7)], and D. Mukai[(8)]

[(1)] *Professor, Tokyo Institute of Technology, Japan, kono.s.ae@m.titech.ac.jp*
[(2)] *Researcher, Building Research Institute, Japan, t_mukai@kenken.go.jp*
[(3)] *Senior fellow, Fujita Corporation, Japan, katsumi.kobayashi@fujita.co.jp*
[(4)] *Professor, Hiroshima Institute of Technology, Japan, o.kaneko.b8@cc.it-hiroshima.ac.jp*
[(5)] *Professor, Shibaura Institute of Technology, Japan, skishida@shibaura-it.ac.jp*
[(6)] *Senior fellow, Taisei Corporation, Japan, komuro@arch.taisei.co.jp*
[(7)] *Assistant Professor, Tokyo Institute of Technology, Japan, obara.t.ac@m.titech.ac.jp*
[(8)] *Associate professor, University of Wyoming, USA, dmukai@uwyo.edu*

Abstract

Seismic design of piles and foundations in Japan is based on working stress concept for minor and intermediate scale earthquakes even if seismic design of upper structural system of buildings has been gradually moving toward the performance based design. The legislature does not require consideration of the ultimate state of piles and foundations for severe earthquakes, mainly because very few buildings have collapsed due to damage to piles and foundations and the study on these structural members has been left out from the main stream of seismic engineering for many years. The issue is even difficult due to the complexity and uncertainty of surrounding soil and boundary conditions of piles and foundations.

Some buildings, however, were demolished after damage to piles in the 1995 Kobe earthquake and 2011 Tohoku earthquake. The Japanese engineers and researchers started to study the ultimate flexural/shear behavior including load carrying capacity and deformation capacity of piles and foundations in order to use buildings continuously even after severe earthquakes.

There are various design issues on cast-in-place piles, precast concrete piles, and pile caps, and it is not easy to make regulations or design guidelines for ultimate conditions. Engineers evaluate the seismic behavior of piles and foundations based on existing knowledge for beams, columns, beam-column joints, and sometimes unavoidably underestimate load bearing and deformation capacities for safety reason since there is not enough experimental data to explain their ultimate behavior under different axial load levels.

Real scale test under large axial load level is very important to study seismic behavior of piles and foundations in order to design them with a performance based design concept. However, very few experimental works have been conducted to clarify the ultimate behavior of these members. The paper introduces recent Japanese efforts to build experimental data on real scale or large scale concrete piles (prestressed high strength spun concrete piles, prestressed high strength reinforced spun concrete piles, steel encased high strength spun concrete piles, cast-in-place reinforced concrete piles, cast-in-place steel encased concrete piles) and foundations (column-beam-pile connections) so that engineers are able to use performance based design concept for piles and foundations.

Keywords: Concrete piles, foundations, damage evaluation, ultimate state, resiliency, performance based design

1. Introduction

Structural design for superstructures has been shifting to the performance based design for multiple levels of ground motions. However, the Japanese design for foundation structures including piles follows a working stress design and does not consider the ultimate conditions. This is because damage to foundations and piles barely caused collapse of superstructures and never lost human lives. In addition, boundary conditions from soil are too complex and uncertain to properly model and design. However, a good number of concrete piles were damaged and some damages lead to demolition of buildings in the 1995 Hyogoken Nanbu Earthquake and the 2011 Miyagi Off-Pacific earthquake. It is urgent to study the ultimate flexure and shear behavior of concrete piles and pile caps with respect to load carrying capacities and deformation capacities so that the performance based design is implemented for foundations and piles and buildings is used continuously after major earthquakes.

Studies have not clarified the seismic behaviors of cast-in-place concrete piles, precast concrete piles, and pile caps. In order to implement performance based design method for the ultimate conditions, experiment should be conducted to build sufficiant data. Effect of axial load level on the ultimate behaviors of piles and pile caps is one of the critical issues to be stated but the current code does not clearly address those issue.

It is necessary to build up experimental data on real or large scale specimens to properly understand seismic behavior of piles and pile caps. However, the experimental studies on piles and pile caps focusing on their ultimate behavior have been scarce. Last several years, large scale experimental studies have been conducted in Japan and the ultimate behavior of piles and pile caps have been gradually clarified. Their ultimate behavior such as flexure capacity, shear capacity, and deformation capacity, under tensile and high compression loads are very practical and important problems in order to secure continuous use of buildings. This paper introduces these large-scale experimental works and their major results on piles and pile caps under tensile or high copressive load.

2. Flexural behavior of concrete piles

This chapter introduces experimental studies on flexural behavior of concrete piles which includes precast spun concrete piles (SC piles, PHC pile, and PRC piles), cast-in-place reinforced concrete piles with or without steel encasing.

2.1 Steel encased precast spun concrete (SC) piles / Precast reinforced spun concrete (PRC) piles

Kaneko et al.[1] summarized test results of 198 precast spun concrete pile specimens which were conducted to study their bending performance. The diameter ranged from 0.3 m to 1.2m and coverd majority of available commercial products. Unfortunately, all data cannot be used for academic purposes since some specimens have only nominal or design dimensions and material properties but did not have measured mechanical properties of materials and/or geometric information of specimens such as concrete strength, concrete thickness, steel strength. They are valuable data to see the bending performance of precast spun concrete piles, but many specimens had no or small axial load and the behavior under large earthquake motions was not clarified.

Nagasawa et al. [2] tested 7 SC piles and 6 PRC piles under cantilever type loading configuration to quantify flexural capacity and deformation capacities under various axial load levels as shown in Table 2 and Table 3. Static cyclic loading was applied using a cantilever type loading system as shown in Figure 1(a).

- Drift of axial force carrying capacity of SC piles depended on the axial force level and the presence of infill in the hollow portion. A simple fiber based section analysis may underestimate the bending moment capacity for high axial load ratio and thin concrete as shown in Figure 2.

- The axial force carrying capacity of PRC piles was completely lost at the end of the loading. The drift for this critical event happened sooner after the peak as the axial force level increased. The infill in a hollow portion of PRC piles is not as effective for ductility as that for SC piles.

Table 1 Number of specimens tested in the precast spun concrete pile industries [1]

Pile type	Pile diameter D (m)											
	0.3	0.35	0.4	0.45	0.5	0.6	0.7	0.8	0.9	1.0	1.1	1.2
PHC	0	0	5	1	1	10	10	5	0	0	1	2
PRC	4	0	47	1	2	16	1	3	0	8	0	0
PC	0	21	0	0	4	0	0	0	0	0	0	0
SC	4	0	29	0	1	11	4	4	1	1	0	1

PHC: Prestressed high strength concrete spun pile, PRC: Prestressed reinforced high strength concrete spun pile, PC: Prestressed concrete spun pile, SC: Steel encased high strength concrete spun pile

Table 2 Major test variables for seven SC pile specimens [2]

Pile	steel casing					concrete layer				Axial load applied N (kN)	Axial load ratio η *2	Filling in hollow section
	Thickness ts (mm)	Yield Stress fy (MPa)	Tensile strength fu (MPa)	Young's modulus Es (GPa)	ts/D *1	Thickness tc (mm)	Compressive strength fc (MPa)	Young's modulus Ec (GPa)	tc/D *1			
SC1	6.0	505	600	212	0.015	66	115	45.6	0.17	0	0.0	Hollow
SC4	6.0	505	600	212	0.015	63	111	44.2	0.16	2,000	0.18	Hollow
SC5	6.0	505	600	212	0.015	68	115	45.6	0.17	3,000	0.26	Hollow
SC6	6.0	505	600	212	0.015	52	115	45.6	0.13	3,500	0.35	Hollow
SC7	4.5	453	545	207	0.011	62.5	115	45.6	0.16	2,000	0.20	Hollow
SC8	6.0	408	492	201	0.015	68	122	46.7	0.17	3,500	0.27	Cement
SC9	6.0	408	492	201	0.015	68	122	46.7	0.17	3,500	0.28	Concrete

*1: All specimens had outer diameteter (D) of 400mm. *2: For hollow piles $N_{max} = A_c f_c + A_s f_y$, for core filled piles $N_{max} = A_c f_c + A_s f_y + A_{cf} f_{cf}$, where A_c, A_s and A_{cf} are the areas of concrete, steel and filling layers, respectively. Compressive strength (f_{cf}) and Young's modulus of filling material for SC8 (cement mortar) were 27.4MPa and 9.95GPa, and those for SC9 (concrete) were 23.7MPa and 26.7GPa.

Table 3 Major test variables for six PRC pile specimens [2]

Pile	Concrete layer				Longitudinal reinforcement			Axial load applied N (kN)	Axial load ratio η *2	Filling in hollow section
	Thickness tc (mm)	Compressive strength fc (MPa)	Young's modulus Ec (GPa)	tc/D *1	Number and Size	Yield strength fsy (MPa)	Tensile strength fsu (MPa)			
PRC01	75.3	116	48.3	0.17	8-D16	372	536	0	0.00	Hollow
PRC02	75.6	112	48.8	0.16	8-D16	372	536	2,000	0.27	Hollow
PRC03	76.3	116	48.4	0.17	8-D16	372	536	3,000	0.40	Hollow
PRC04	75.0	123	49.9	0.13	8-D13	385	536	3,000	0.41	Hollow
PRC05	78.0	115	44.5	0.16	8-D22	370	534	2,000	0.26	Concrete
PRC06	76.5	125	47.7	0.17	8-D16	372	536	3,000	0.40	Hollow

*1: All specimens had out diameteter (D) of 400mm and 8-ϕ10 prestressing tendons. Yield strength (f_{py}) and tensile strength (f_{pu}) for prestressing tendons were 1331MPa and 1404MPa, respectively. For hollow piles $N_{max} = A_c f_c + A_s f_y + A_p f_{py}$, for core filled piles $N_{max} = A_c f_c + A_s f_{sy} + A_p f_{py} + A_{cf} f_{cf}$, where A_c, A_s, A_p and A_{cf} are the areas of concrete, longitudial reinforcement, prestressing reinforcement, and filling, respectively. Compressive strength (f_{cf}) and Young's modulus of filling material for PRC05 were 22.8Mpa and 25.7GPa.

Asai et al. [3] carried out bending test on 42 simply supported precast spun concrete piles in order to study their bending performance under tensile and/or high compressive axial force. Piles under low axial force were tested at six factory laboratories and those under tensile and high compressive axial force were tested at BRI as shown in Figure 1(b). They included 8 SC piles (N/N_{max}=-0.4 – 0.52), 17 PRC piles (N/N_{max}=-0.25 – 0.41), and 17 PHC piles (N/N_{max}=-0.26 – 0.43). The major test variables were type of piles (SC, PRC, and PHC piles), loading protocol (one-directional cyclic loading, reversal cyclic loading), and axial load force ratio. The following conclusions were drawn.

- SC piles reached the ultimate condition before the steel encasing had local buckling. As the axial force ratio increased, deformation capacity decreased. The axial load carrying capability was maintained even after the bending moment capacity was reached.
- PRC and PHC piles had brittle failure with very poor deformation capacity when axial compressive force ratio was over 0.4. PHC piles were not able to sustain tensile force after they failed due to fracture of prestressing tendons if the axial tensile force was as low as -0.25. Under same loading conditions, however, PRC piles sustained their tensile force since longitudinal mild steel reinforcement carried all tensile force after fracture of prestressing tendons.
- Moment – curvature relations of piles (SC, PHC, and PRC) can be reproduced with a section analysis assuming “a plane section remains plane”. With better stress – strain relation models for confined concrete and prestressing tendons, the moment – curvature relation is simulated with higher accuracy.

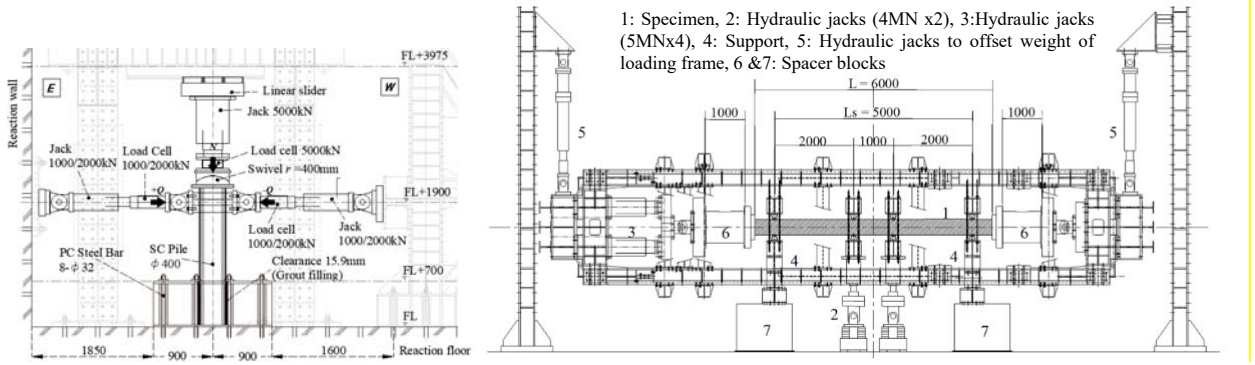

(a) Copita loading system has 5MN capacity [2] (b) System has 20MN capacity at Building Research Institute [3]

Figure 1 Loading setup (Unit: mm)

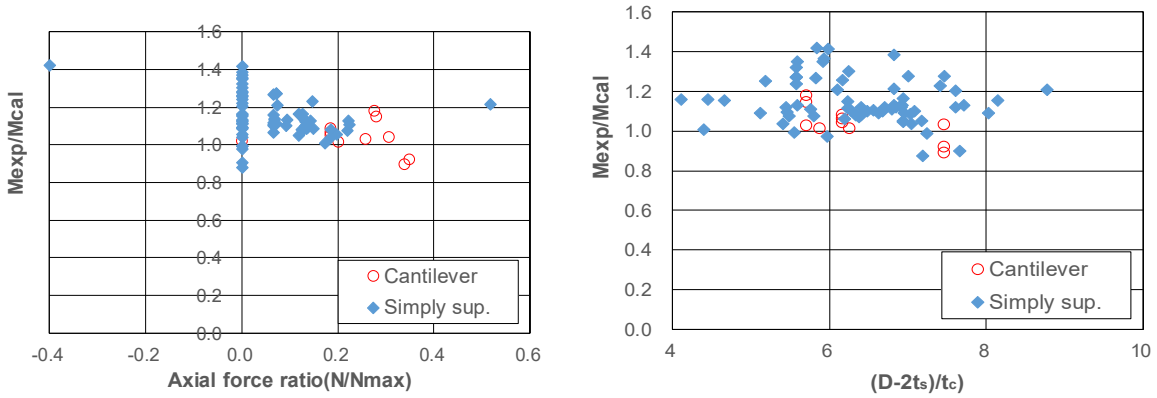

(a) Axial force ratio (b) Ratio of concrete out diameter and concrete thickness

Figure 2 Ratio of experimental and computed moment capacity for SC piles (limit strain was set to 0.004)

2.2 Cast-in-place reinforced concrete piles

Nakamura et al.[4] tested twelve 1/3-scale cantilevered cast-in-place RC pile specimens. Three of them were retrofitted specimens with mortar or steel plate jacketing. Test variables were shear span to depth ratio, and axial force ratio (-0.20 – 0.40) as shown in Table 4 and Figure 3.

- Piles with flexural failure mode had higher stiffness and lateral load carrying capacity and lower ultimate deformation capacity as the axial load ratio increased.
- Piles with shear failure mode had abrupt drop of load carrying capacity after reaching the peak at R=1.0%.
- Backbone curves including shear and moment capacities of piles can be conservatively estimated with the existing formulae for RC columns.
- Retrofitted piles were able to gain enhanced stiffness and capacities by proper retrofit scheme with steel jacketing and ample anchorage length of longitudinal reinforcement.

Table 4 Major test variables for Cast-in-place reinforced concrete piles [4]

No.	Specimen	Shear span to depth ratio	Axial force ratio η
1	N-3L	3.0	0.15
		2.0	0.40
2	N-2S	2.0	0.40
3	N-2L		0.15
4	V-2		0 to 0.40
5	N-1.75S-I	1.8	0.40
6	N-1.75S-C		
7	V-1.75		-0.20 to 0.40
1−2	N-3L-R	3.0	0.15
2−2	N-2S-R	2.0	0.15
3−2	N-2L-R		
8	N-1.4S-H	1.4	0.40
9	N-1.4S		

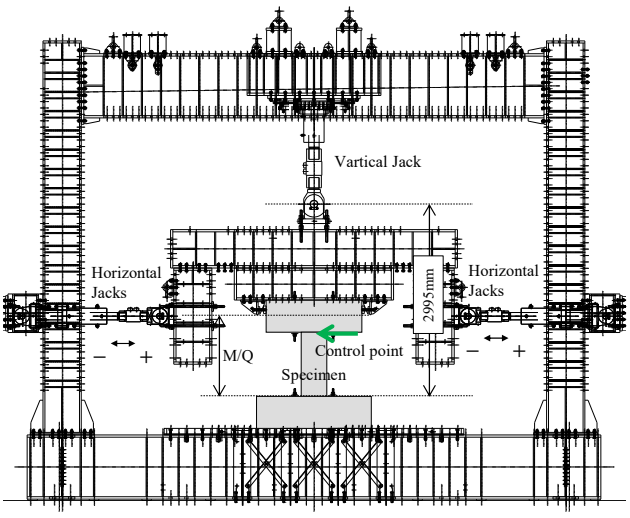

Figure 3 Loading setup for bending/shear test for RC piles at Building Research Institute (Unit: mm) [4]

Suguyam et al. [5] tested 7 reinforced concrete specimens with 800mm diameter, 60MPa class concrete under low to high axial force ratio as shown in Table 5 and Figure 4. Seven specimens had identical dimension and reinforcement but different axial force ratio. Specimens were loaded under anti-symmetric moment distribution condition as shown in Figure 4(b) Axial load was kept constant for three specimens (No.1, 4, and 6) and varied along with lateral load for remaining four specimens (No.2, 3, 5, and 7) as shown in Figure 4(c). As shown in Figure 5, all specimens failed and lost their axial load carrying capacity when longitudinal reinforcement buckled after fracture of shear reinforcement following crushing of concrete at flexure compression zone. The drift ratio at failure for η=0.25 (No. 1, No. 4, and No.6) was more than 2 %. That for η=0.4 - 0.5 (No. 2, No. 5, and No.7) was larger than 1% but smaller than 1.5%. The ultimate drift capacity was poor for larger axial force ratio. The transition axial force ratio from ductile to brittel decreased as concrete strength increased. Moment – curvature relation was simulated with a simple section analysis. It was reported that the maximum moment and ultimate curvature was overestimated for specimens with f'c=90MPa (No.6 and No.7).

Table 5 Major test variables for Cast-in-place reinforced concrete piles [5]

No.	Major variables					Test results	
	Compressive strength of concrete σ_B (N/mm^2)	Longitudinal reinforcement ratio p_g (%)	Shear reinfocement ratio p_w (%)	Axial force ratio η	Axial force N (kN)	Max. shear force Q_{exp} (kN)	Q_{exp}/Q_{cal}
1	66.8	1.03 (18-D19) (SD390)	0.2 (U9.0@80) (SBPD1275/1420)	0.25	8390	1750	1.02
2	62.7			0.50～0.0	15760～0	1820	1.16
3	67.5			0.40～0.10	13570～3390	1850	0.95
4	43.1			0.25	5420	1317	1.08
5	43.9			0.5～0.0	11040～0	1487	1.26
6	91.0			0.25	11440	2142	0.97
7	96.0			0.40～0.10	19310～4830	2293	0.87

$p_g=a_g/A_c$, a_g: total section area of longitudinal reinforcement, A_c:Gross area of pile and $A_c=\pi \cdot D^2/4$, D: pile diameter
$p_w=a_w/(D \cdot x)$, a_w: total section area of a set of shear reinforcement, x: spacing of shear reinforcement, $N=\eta A_c \sigma_B$
Qcal was computed with a section analysis.

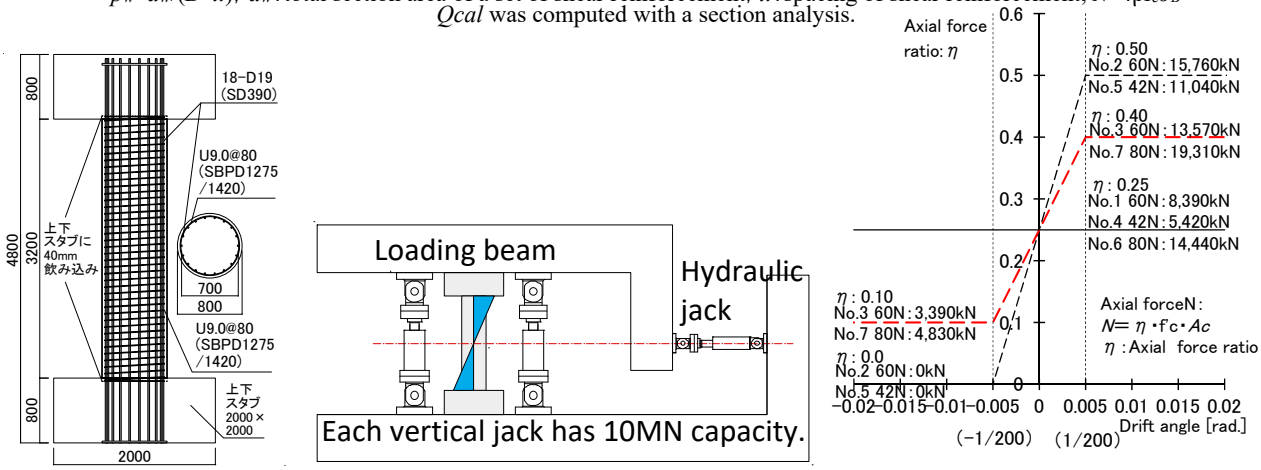

(a) Specimen (b) loading system (c) Loading path

Figure 4 Pile specimen for bending/shear test at Taisei corporation (Unit: mm) [5]

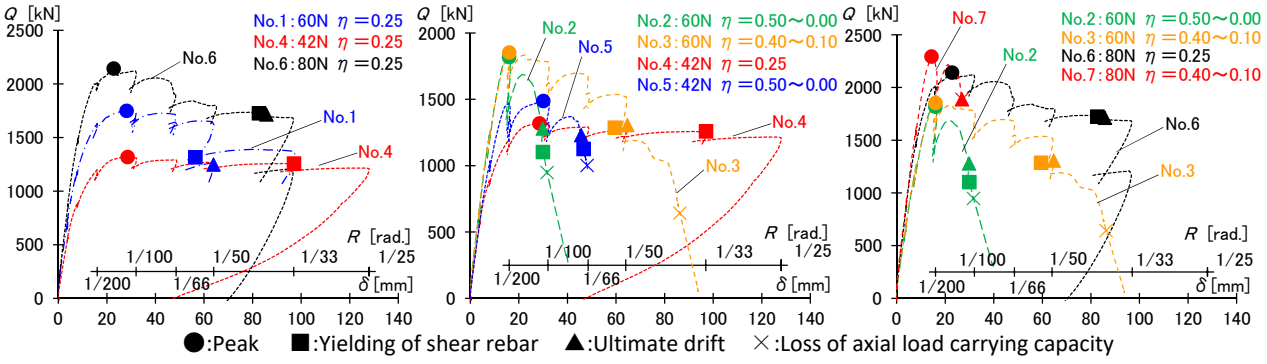

Figure 5 Load (Q) – drift ratio (R) envelop curves [5]

2.3 Steel encased cast-in-place concrete piles

Tanaka et al. [6] carried out flexural test on steel encased cast-in-place concrete piles to study their ultimate behavior. The piles had diameter (D) of 1200mm and steel casing thickness (t_s) of 9.6 mm, with and without longitudinal reinforcement. They had diameter to steel encasing thickness ratio (D/t_s) of 125, which is relatively large for experimental specimen although it is not large enough compared to real piles of this kind.

Major vaiables of specimens are shown in Table 6. (a) Load path (b) Loading system in BRI (Photo of Figure 1(b))

Figure 6 shows the loading path and the loading system in BRI.

- All five specimens reached the ultimate condition by local buckling after the peak point, followed by the fracture of that portion for some specimens. The axial load carrying capacities were maintained after the failure.
- Backbone curve including yield and peak points can be estimated from a simple section analysis although assumption of "a plane section remains plane" is questionable for these piles.

Table 6 Major test variables for pile and pile cap assemblages [6]

Specimen	SC-TB1	SC-TB2	SC-TB3	SRC-TB1	SRC-TB2
D/ts	125	125	125	125	125
Shear span to diameter ratio(M/QD)	2.5	2.5	2.5	2.5	2.5
Long. Reinforcement	-	-	-	12-D32	12-D32
type of long. rebar	-	-	-	SD390	SD390
Long. Rebar ratio(Pg) (%)	-	-	-	0.84	0.84
Gross area of long. rebar (A_m) (mm^2)	0	0	0	9530	9530
Converted concrete area (A)	1,378,052	1,390,450	1,405,492	1,400,941	1,401,803
Initial axial load N_s (N/N_0) (kN)	4070 (0.09)	4070 (0.09)	4070 (0.09)	4070 (0.09)	4070 (0.09)
Max. axial load N_{max}(N/N_0) (kN)	6786 (0.15)	13572 (0.31)	18661 (0.43)	18993 (0.41)	6786 (0.15)
Min. axial load N_{min}(N/N_0) (kN)	-3299 (-0.21)	-3299 (-0.21)	-3299 (-0.21)	!-4172 (-0.21)	-3299 (-0.17)

Five specimens had the following quantities in comment. Pile diameter(D) = 1200mm, pile length (L)= 8000mm, steel casing thickness (ts)=9.6mm, steel casing type: SKK490, section area of steel casing (As) = 35902mm2, Concrete section area (Ac)=1,095,072mm2

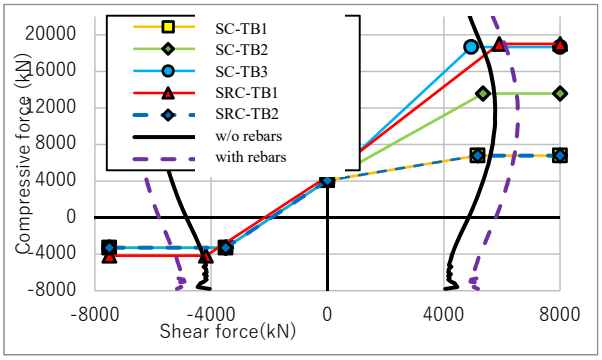

(a) Load path (b) Loading system in BRI (Photo of Figure 1(b))

Figure 6 Load path on axial force and shear force relation [6]

3. Shear behavior

3.1 PHC piles and PRC piles

Otaki et al. [7] carried out shear test on three PHC piles and six PRC piles as shown in Figure 7 and Table 7. Constant axial load was applied using loading system in Figure 1. Central two hydraujacks were loaded with same magnitude but in opposite direction. Major variables were shear span to diameter ratio (1.4 and 2.1), and axial force ratio (ranging from -0.26 to 0.34).

PHC piles under high axial load (N/Nmax=0.13 and 0.27) and PRC piles with high axial load (N/Nmax=0.23 and 0.34) experienced splitting cracks running parallel to the pile axis followed by brittel failure as shown in

Figure 8(b). PRC piles under tensile force sustained axial force at the ultimate conditions. Shear capacity equation in the 2017 AIJ guidelines [8] overestimated the test results by 15% at maximum. Ishikawa et al. [8] compared the shear capacity equations of the 2017 AIJ guidelines and additional 223 test results (97 PHC piles and 126 PRC piles) from database.

- As axial load increased, the failure mode changed from diagonal shear crack failure (Figure 8(a)) to splitting crack failure (Figure 8(b)).
- Average and coefficient of variation of $_{exp}Q_{SU}/_{AIJ}Q_{SU}$ were 1.24 and 0.22 (defect ratio of 13%) for PHC piles and 1.17 and 0.18 (defect ratio of 11%) for PRC piles. Value $_{exp}Q_{SU}/_{AIJ}Q_{SU}$ decreases as axial force ratio increases for both PHC and PRC piles as shown in Figure 9.

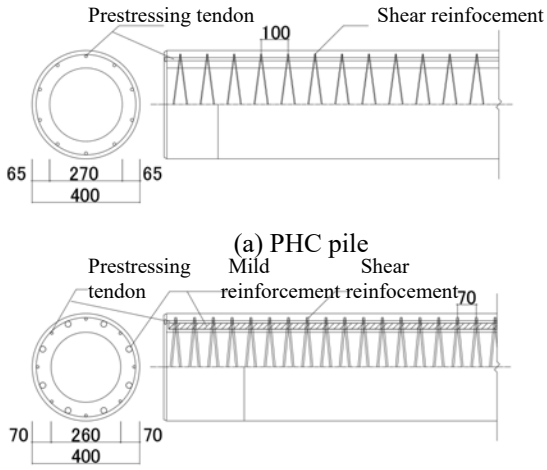

Figure 7 Piles tested in shear loading [7]

Table 7 Major test variables for shear test on PHC and PRC piles [7]

Specimen	PHC18	PHC19	PHC20	PRC27	PRC28	PRC29	PRC24	PRC25	PRC26
Diameter D and Thickness of steel encasing ts (mm)	400 and 6.0								
Thickness of concrete (mm)	70.1	71.3	69.5	74.6	77.4	77.7	75.2	74.2	77.4
Mild reinforcement,	None			8-D22					
Prestressing tendon and shear reinfocement	10-ϕ 11.2			8-ϕ 10.0					
Shear reinforcement	ϕ 3.2@100			ϕ 6.5@70					
Axial force, Nmax (kN)	-344	1368	2752	-510	1655	4137	-196	1655	2731
N/Nmax	-0.26	0.13	0.27	-0.1	0.14	0.23	-0.25	0.13	0.34
Shear span to diameter ratio M/QD	1.4						2.1		
Concrete compressive strength (MPa)	116	117	114	124	132	129	119	127	121

※1 : N is positive under compression. ※2 : $\sigma o=N/((A-Ap-Ad)+Ap \cdot (Ep/Ec)+Ad \cdot (Ed/Ec))$ where A: Measured section area, Ap and Ep: Total section area and Young's modulus of prestressing tendons, Ad and Ed: Total section area and Young's modulus of deformed mild reinforcement, Ec: Young's modulus of concrete. ※3 : $N/N_0=N/(\sigma B \cdot (A - Ap - Ad)+fpy \cdot Ap+fdy \cdot Ad)$ (for N>0) , $N/N_0=N/(fpy \cdot Ap+fdy \cdot Ad)$ (for N<0) (where fpy and fdy: Yield strengths of prestressing tendons and deformed mild reinforcement.

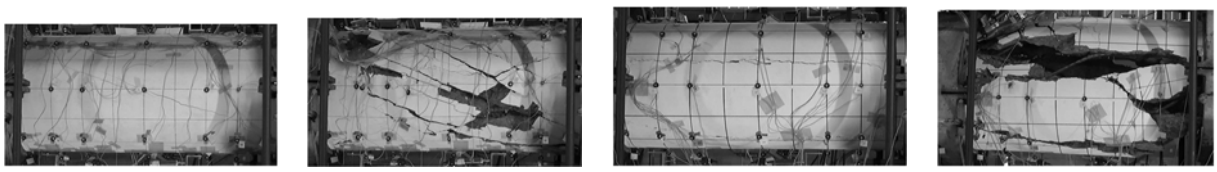

(a) PRC28 with intermediate axial force (N/Nmax=0.14) (b) PHC20 with high axial force (N/Nmax=0.27)

Figure 8 Crack patterns for peak (left) and ultimate (right) [7]

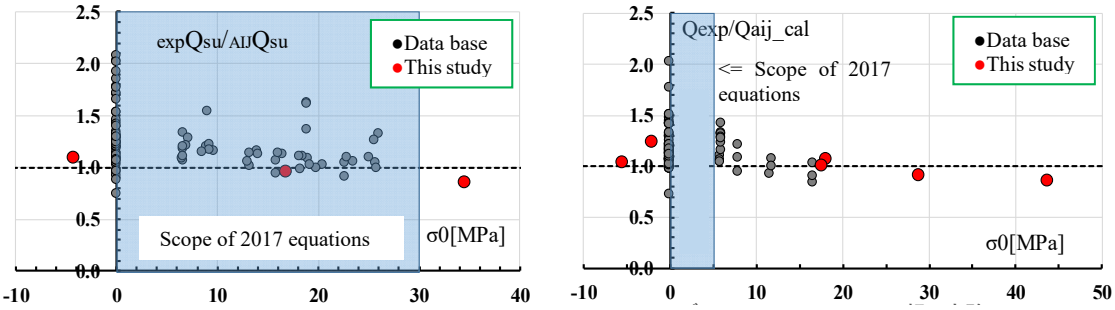

(a) PHC piles (b) PRC piles

Figure 9 $_{exp}Q_{SU}/_{AIJ}Q_{SU}$ and axial stress relations (σ_0 does not include prestressing stress) [8]

4. Pile cap

Chihama et al. [10][11] carried out experiment on two pile and pile cap assemblages as shown in Figure 10 in order to study bending behavior. Axial load was varied as a function of beam shear force. Four specimens had different amount of anchorage reinforcement and two kinds of pile (steel encaase spun concrete pile and steel encased cast-in-place pile) so that the different failure modes (flexure and shear) can be observed.

- SP1 and SP2 reached the ultimate condition when the concrete under flexural compression zone failed in compression for SP1 and pile cap failed in shear for SP2. However, the obtained capacities in positive side were obtained from section analysis assuming two times bearing capacity. Tested was carried out until R=+2.5% for No.1 and R=-4.5% for No.2. Two specimens could have deformed further from damage states.
- TS1 failed at the pile-pile cap interface and TS2 faile at the pile. Obtained M-ϕ relation at the interface was not properly simulated with a simple section analysis and further study is needed.

Kishida et al. [12] conducted a series of experiment to study shear resisting mechanisms and ultimate shear capacity of pile caps. Some specimens had an offset column or a column with side wall with different configuration of reinforcement arrangement in a pile cap under different level of axial force ratio to make realistic boundary conditions. Unfortunately, the space is limited to fully describe their interesting results in this paper.

- Current practice of reinforcement arrangement is not necessarily efficient. Rational reinforcement arrangement should be considered based on shear resisting mechanism, although it is not fully clear at this moment.
- Shear resisting mechanism change depending on presence of walls and offset of columns.
- Axial force level is one of the important variables affecting on the shear resisting mechanism of pile caps.

Table 8 Major test variables for specimens with SC pile [10] [11]

Specimen		SP1	SP2	TS1	TS2
Pile type		Steel encased spun concrete pile		Steel encased cast-in-place pile	
Axial force ratio (N/N0)		-0.4 ~ +0.54	-0.4 ~ +0.36	-0.4 ~ +0.54	+0.36
Column	B×D	720mm×720mm		1100mm×1000mm	
	Long. reinf.	12-D32(SD390)		24-D32(SM490C)	
Foundation beam	B×D	900mm×2000mm		900mm×2000mm	
	Long. reinf.	16-D32(SD390)		24-D32(SM490C)	
Pile	SC pile	ϕ 400, t=21mm, SSK490, f'c105MPa		ϕ 800, t=9.8mm, f'c40MPa	
	Anchor reinf.	8-D29(SD345)	14-D38(WSD490)	18-D35(WSD490)	
Pile cap	f'c	21MPa		40MPa	
	B×D×H	900mm×900mm×2350mm		1200mm×1200mm×2255mm	
	Vert. reinf.	8-D13(SD295A)		40-D22(SD345)	
	Web reinf.	D10(SD295A) @185		12-D16(SD295A)	

N/N0:Axial force ratio B, D, and H: width, length, and height SC pile: Steel encased spun concrete pile

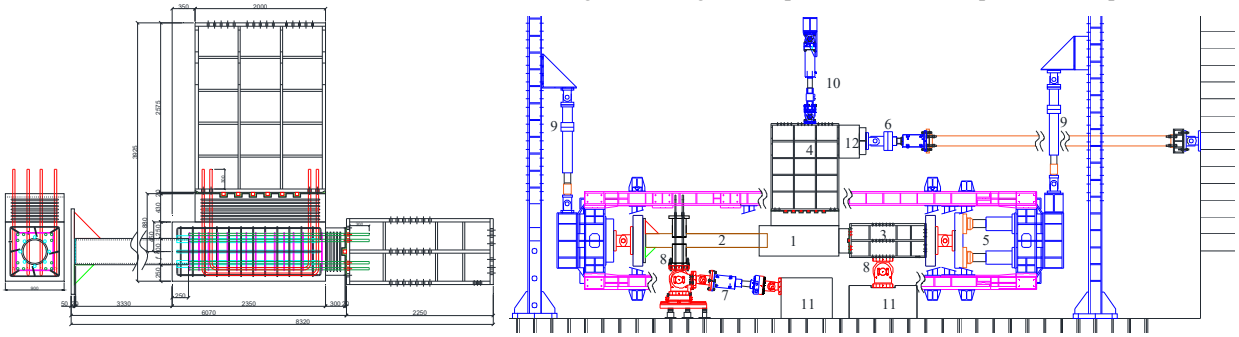

(a) SP1 (b) Loading system in BRI

Figure 10 Pile and Pile cap assemblage specimen and loading system [10]

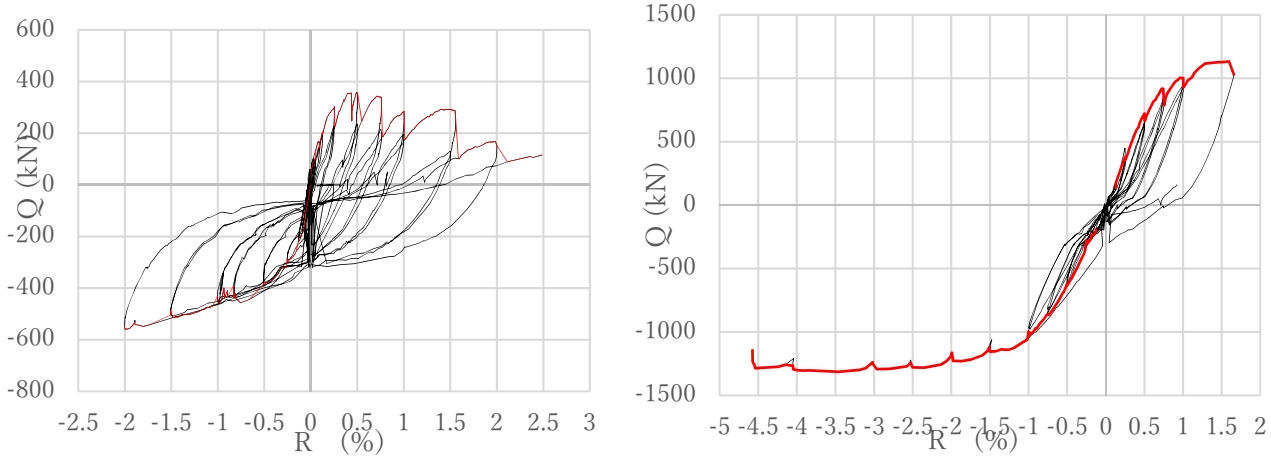

(a) Load – drift ratio relation for SP1 (b) Load – drift ratio relation for SP2

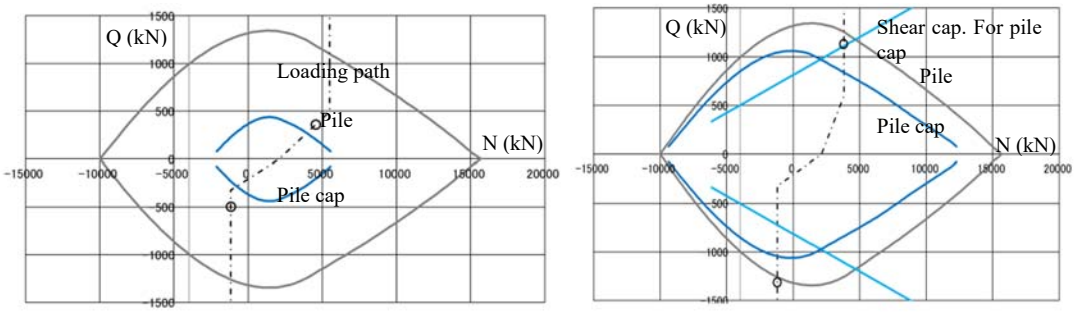

(c) Load path and capacity for SP1 (b) Load path and capacity for SP2

Figure 11 Test results for pile-pile cap specimens [10]

5. Conclusions

Series of experiments on concrete piles (Cast-in-place piles and precast concrete piles) and pile caps were reported to clarify their behavior for different limit states, focusing on the ultimate conditions. Test variables were chosen to expand the scope of knowledge with respect to load carrying capacity and ultimate deformation. Based on recent experimental data, the causes have been bocoming clarified for damages to piles observed after the 1995 Kobe earthquake. The study will enhance the understanding of their seismic behavior in order for structures to be used continuously after earthqueakes for better resilience. Based on the experimental results reported in this paper, some changes are expected as listed in Table 9. Readers who are interested may want to see document in Ref. [13] which has more detailed description of some experiments.

There are still many issues to be solved and major ones are listed below.

- Issues related to flexural behavior of piles include confinement effect of concrete for precast concrete piles (PHC, PRC, and SC piles), and buckling behavior of steel casing for steel encased concrete piles for both cast-in-place and precast piles. The current ultimate flexural capacity equations have tendency of overestimation for all piles as the compressive axial load ratio increases. Concrete dominant piles such as PHC/PRC piles needs consideration on size effect. Knowledge on flexural deformation of pile is quite limited and needs more study.
- Shear behavior of PHC/PRC piles needs more attention. Their failure under high axial force ratio is caused by the longitudinal splitting crack of piles and this needs further study. Safety margin of the AIJ shear

capacity equation decreases as compressive axial force increases. Knowledge on shear deformation of pile is quite limited and needs more study.

- Flexural behavior at the pile-pile cap interface and shear behavior of pile cap need clarification of resisting mechanism and proper capacity equation should be proposed.

Table 9 Expected major changes in AIJ guidelines

Fabrication	Pile type	Design issue	Before experiment (2017 AIJ Guidelines)	After experiment (2021 AIJ Guildelines)
Cast-in-place	RC pile	Flexure/shear capacities	N/Nmax=-0.05～1/3	→ N/Nmax=-0.1～0.6 (expanded)
		Deformation	Ru=1/100	→ Ru for axial load carrying capacity is shown
	Steel encased (reinforced) concrete pile	Flexure capacity	N/Nmax=-0.07～0.15	→ N/Nmax=-0.3～0.55 (expanded)
		Deformation	equation without validation	→ Limit deformations is included
		Width to thickness ratio	less than 100	→ less than 133 (expanded)
Precast	PHC pile	Flexure/shear capacities	N/Nmax=0～0.3	→ N/Nmax=-0.05～0.4 (expanded)
	PRC pile	Flexure/shear capacities	N/Nmax=0～0.05	→ N/Nmax=-0.25～0.4 (expanded)
		Deformation	equation without validation	→ Ru for axial load carrying capacity is shown
	SC pile	Flexure capacity	no equation	→ N/Nmax=-0.1～0.5
		Deformation	no equation	→ Limit deformations is included

* N/Nmax:Axial force ratio, Ru: limit drift ratio, the 2017 AIJ guidelines was published in March 2017, and the 2017 AIJ guidelines is under review and expected to publish in 2021.

6. Acknowledgements

The work was supported financially by JSPS through two Grant-in-Aid programs (PI: Shuji Tamura, and Susumu Kono). We are thankful to the Concrete Pile and Pole Industrial Technology Association and Steel encased Cast-in-place Concrete Piles Association for their expert advice and support. We are also thankful to the Consortium for Socio-Functional Continuity Technology supported by JST Program on Open Innovation Platform with Enterprises(JPMJOP1723), the Collaborative Research Project (Materials and Structures Laboratory) and the World Research Hub Initiative (Institute of Innovative Research) at Tokyo Institute of Technology for their generous support of this work.

Large amount of information in this paper was obtained from the following projects and we are thankful to those who worked on the projects.

- Housing and Building Technology Enhancement Project (2015 – 2017 Ministry of Land, Infrastructure, Transport and Tourism)
- Long-life building system promotion project (2016 – 2017 Ministry of Land, Infrastructure, Transport and Tourism)
- Study on structural performance evaluation for concrete pile sub-assemble system with post-earthquake functional use (Building research institute)

7. References

[1] Kaneko, Nakai, Mukai, Iiba, Hirade, and Abe: The Flexural Strength And Deformation Characteristics Of Precast Concrete Piles For Estimation Of Seismic Performance Against Severe Earthquakes, J. of Technology Design, Vol. 21, No. 47, pp. 95-98, 2015.
[2] Nagasawa et al.: Study on flexural deformation of precast concrete piles, Summaries of technical papers of annual meeting AIJ, pp. 757- 764, 2016.
[3] Asai et al.: Study on structural performance evaluation for concrete pile system with post-earthquake functional use (Part 2 – 5), Summaries of technical papers of annual meeting AIJ, pp. 577-584, 2017.
[4] Nakamura et al. : Study on structural performance evaluation for concrete pile system with post-earthquake functional use (Part 12), Summaries of technical papers of annual meeting AIJ, pp. 597-598, 2017.
[5] Sugiyama et al. : Seismic Performance of Cast-in-place Concrete Pile (Part 1 – 4), Summaries of technical papers of annual meeting AIJ, pp. 573 – 576, 2018. and pp. 197 – 200, 2019.
[6] Tanaka et al.: Study on structural performance evaluation for concrete pile system with post-earthquake functional use (Part 6&7), Summaries of technical papers of annual meeting AIJ, pp. 585-588, 2017.
[7] Otaki et al.: Study on structural performance evaluation for concrete pile system with post-earthquake functional use (Part 8&9), Summaries of technical papers of annual meeting AIJ, pp. 589-592, 2017
[8] Ishikawa et al. : Shear Strength Evaluation Based on Shear Experiment Database of PHC and PRC Piles, Summaries of technical papers of annual meeting AIJ, pp. 615-618, 2018.9
[9] Architectural Institute of Japan: AIJ Guidelines for Seismic Design of Reinforced Concrete Foundation Members (Draft), 2017
[10] Chihama et al.: Study on structural performance evaluation for concrete pile system with post-earthquake functional use (Part 22&23), C2, pp. 589-592, 2018.
[11] Imai et al.: Study on structural performance evaluation for concrete pile system with post-earthquake functional use (Part 21), C2, pp. 587-588, 2018.
[12] Kishida et al.: Study on structural performance evaluation for concrete pile system with post-earthquake functional use (Part 13 – 15), Summaries of technical papers of annual meeting AIJ, pp. 599- 604, 2017.
[13] Mukai et al.: Study on Structural Performance Evaluation for Concrete Pile Sub-assemble System with Post-earthquake Functional Use, Building Research Institute, 2019.

